Available online at www.sciencedirect.com
SCIENCE DIRECT®
Chemical Physics Letters 393 (2004) 51–57
CHEMICAL PHYSICS LETTERS
www.elsevier.com/locate/cplett

A new hybrid exchange–correlation functional using the Coulomb-attenuating method (CAM-B3LYP)

Takeshi Yanai [a,*], David P. Tew [b], Nicholas C. Handy [b]

[a] Oak Ridge National Laboratory, P.O. Box 2008, MS6367, Oak Ridge, TN 37831, USA
[b] Department of Chemistry, University of Cambridge, Cambridge, CB2 1EW, UK

Received 15 March 2004; in final form 4 June 2004

Abstract

A new hybrid exchange–correlation functional named CAM-B3LYP is proposed. It combines the hybrid qualities of B3LYP and the long-range correction presented by Tawada et al. [J. Chem. Phys., in press]. We demonstrate that CAM-B3LYP yields atomization energies of similar quality to those from B3LYP, while also performing well for charge transfer excitations in a dipeptide model, which B3LYP underestimates enormously. The CAM-B3LYP functional comprises of 0.19 Hartree–Fock (HF) plus 0.81 Becke 1988 (B88) exchange interaction at short-range, and 0.65 HF plus 0.35 B88 at long-range. The intermediate region is smoothly described through the standard error function with parameter 0.33.

1. Introduction

In density functional theory (DFT), as it is used for computational chemistry, the hybrid functional B3LYP [2,3] appears to offer the greatest contribution (if measured by the number of applications which have been published). However it is unsuccessful in a number of important applications: (i) the polarizability of long chains, (ii) excitations using time dependent theory (TDDFT) [4–6] for Rydberg states, and perhaps most important (iii) charge transfer (CT) excitations [7–9]. The reason for these failures is understood, at long-range the exchange potential behaves as $-0.2r^{-1}$, instead of the exact value $-r^{-1}$. Even so, the potential is an improvement over that LDA and BLYP, where there is no r^{-1} dependence in the potential.

Recently Tsuneda and co-workers [1] have overcome this deficiency through an Ewald split of r_{12}^{-1} into

$$\frac{1}{r_{12}} = \frac{1-\mathrm{erf}(\mu r_{12})}{r_{12}} + \frac{\mathrm{erf}(\mu r_{12})}{r_{12}}. \tag{1}$$

The first term accounts for the short-range interaction, and the second term accounts for the long-range interaction. The key in the long-range-corrected (LC) exchange functional scheme for DFT [10–13] is that the DFT exchange interaction is included using the first term (short-range), and the long-range orbital–orbital exchange interaction is described with the Hartree–Fock (HF) exchange integral via the complementary term. Specifically, the short-range part of the exchange interaction is incorporated by modifying the usual exchange functional form, $E_x = -(1/2)\sum_\sigma \int \rho_\sigma^{4/3} K_\sigma \mathrm{d}^3\mathbf{r}$, into

$$E_x^{\mathrm{sr}} = -\frac{1}{2}\sum_\sigma \int \rho_\sigma^{4/3} K_\sigma \times \left\{1 - \frac{8}{3}a_\sigma\left[\sqrt{\pi}\,\mathrm{erf}\left(\frac{1}{2a_\sigma}\right) + 2a_\sigma(b_\sigma - c_\sigma)\right]\right\}\mathrm{d}^3\mathbf{r}, \tag{2}$$

where a_σ, b_σ and c_σ are:

$$a_\sigma = \frac{\mu K_\sigma^{1/2}}{6\sqrt{\pi}\rho_\sigma^{1/3}}, \tag{3}$$

$$b_\sigma = \exp\left(-\frac{1}{4a_\sigma^2}\right) - 1, \tag{4}$$

$$c_\sigma = 2a_\sigma^2 b_\sigma + \tfrac{1}{2}. \tag{5}$$

* Corresponding author. Fax: +1-865-574-0680.
E-mail address: yanait@ornl.gov (T. Yanai).

0009-2614/$ - see front matter © 2004 Elsevier B.V. All rights reserved.
doi:10.1016/j.cplett.2004.06.011

To reach this form, $\mathrm{erfc}(\mu r_{12})$ has been multiplied by the square of the one-particle density matrix for the uniform electron gas, and then integrated [12]. Use of K_σ allows the incorporation of generalized gradient approximation functionals [10]. The long-range part of the exchange interaction is expressed with the HF exchange integral [12],

$$E_x^{\mathrm{lr}} = -\frac{1}{2}\sum_\sigma \sum_i^{occ}\sum_j^{occ} \int\int \psi_{i\sigma}^*(\mathbf{r}_1)\psi_{j\sigma}^*(\mathbf{r}_1) \times \frac{\mathrm{erf}(\mu r_{12})}{r_{12}}\psi_{i\sigma}(\mathbf{r}_2)\psi_{j\sigma}(\mathbf{r}_2)\,\mathrm{d}^3\mathbf{r}_1\,\mathrm{d}^3\mathbf{r}_2, \quad (6)$$

where $\psi_{i\sigma}$ is the ith σ-spin molecular orbital. The parameter μ determines the balance of DFT to HF exchange at intermediate r_{12}. If $\mu = 0$, the LC DFT calculation corresponds to the pure (non-LC) DFT calculation, and conversely $\mu = \infty$ corresponds to the standard HF calculation. Tsuneda and co-workers have demonstrated that their LC method for the Becke 1988 [14] or PBE [15] generalized-gradient approximation (GGA) exchange functionals in conjunction with their one-parameter progressive (OP) correlation functional [16] can address the above notorious problems in DFT. The incorrect long-range exchange interaction delivered by the standard DFT exchange functionals seems to lead to the underestimation of 4s–3d interaction energies of the first-row transition metals, the overestimation of the longitudinal polarizabilities of π-conjugated polyenes, the poor description of the weak interaction of van der Waals bonding of rare-gas dimers, and the underestimations of Rydberg excitation energies, oscillator strengths, and charge-transfer excitation energies. Tsuneda and co-workers have shown that their LC method with $\mu = 0.33$ gives greatly improved results for all of these phenomena [1,10,17].

Unfortunately, we find that LC-BOP does not work well for the more standard energy calculations on which the parameters for B3LYP were derived. Indeed, the mean absolute error in the atomization energies of 53 molecules with the high quality basis sets, augmented cc-pVQZ, increases from 2.5 kcal mol^{-1} (B3LYP) to 9.5 kcal mol^{-1} (LC-BOP), which seriously detracts from the quality of LC-BOP. The purpose of this Letter is to show how it is possible to combine the ideas behind B3LYP and LC-BOP to deliver a functional which has the energetic qualities of B3LYP and the asymptotic qualities of LC-BOP.

2. Coulomb-attenuating method with three parameters

Now, we generalize the form of Eq. (1) using two extra parameters α and β as,

$$\frac{1}{r_{12}} = \frac{1-[\alpha+\beta\cdot\mathrm{erf}(\mu r_{12})]}{r_{12}} + \frac{\alpha+\beta\cdot\mathrm{erf}(\mu r_{12})}{r_{12}}, \quad (7)$$

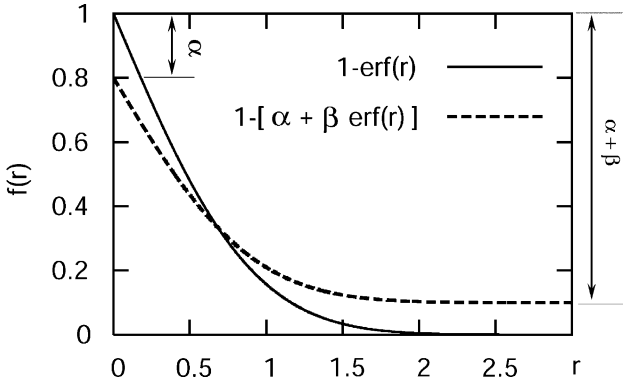

Fig. 1. Plots for $f(r) = 1 - \mathrm{erf}(\mu r)$ and $f(r) = 1 - [\alpha + \beta\mathrm{erf}(\mu r)]$.

where the relations $0 \leqslant \alpha + \beta \leqslant 1$, $0 \leqslant \alpha \leqslant 1$, and $0 \leqslant \beta \leqslant 1$ should be satisfied. We term this the 'Coulomb-attenuating method (CAM)' approach. Fig. 1 illustrates the schematic plots of two functions, Eqs. (1) and (7). The parameter α allows us to incorporate the HF exchange contribution over the whole range by a factor of α, and the parameter β allows us to incorporate the DFT counterpart over the whole range by a factor of $1-(\alpha+\beta)$. We note that the widely-used hybrid B3LYP functional [2,3] takes CAM potential partitioning of Eq. (7) with $\alpha = 0.2$ and $\beta = 0.0$ for the mixing of Slater exchange E_X^{Slater} and the HF exchange E_X^{HF} as follows:

$$E_X^{B3} = (1-\alpha)E_X^{\mathrm{Slater}} + \alpha E_X^{\mathrm{HF}} + c^{B88}\Delta E_X^{\mathrm{B88}}, \quad (8)$$

where the additional term $\Delta E_X^{\mathrm{B88}}$ is Becke's 1988 gradient correction for exchange [14] with the semiempirical parameter $c^{B88} = 0.72$, which Becke obtained by a linear least-square fit to experimental data [2]. Also, the original LC corresponds to the CAM with $\alpha = 0.0$ and $\beta = 1.0$. Figs. 2a–c show the contributions to exchange from r_{12}^{-1}, apportioned into DFT and HF, for B3LYP, LC and CAM methodologies.

The extra flexibility arising from two extra parameters α and β allows us to look at how important the HF exchange contribution is for the short-range region and the DFT counterpart is for the long-range region. In the original form of the LC decomposition (Eq. (1)), either HF or DFT exchange vanishes at $r = 0$ and $r = \infty$.

We note that CAM with the Gaussian-type basis implementation requires the same types of the Coulomb-attenuated and non-attenuated (standard) two-electron integrals [12] as the original LC approach of Eq. (1). The details about modifying the DFT exchange functionals and the HF exchange integral to involve the error function are described in [1,10].

3. Procedure: trial CAM exchange–correlation functionals

In this Letter, we investigate the performance of the Coulomb-attenuating method with several existing GGA functionals. Table 1 summarizes the exchange–

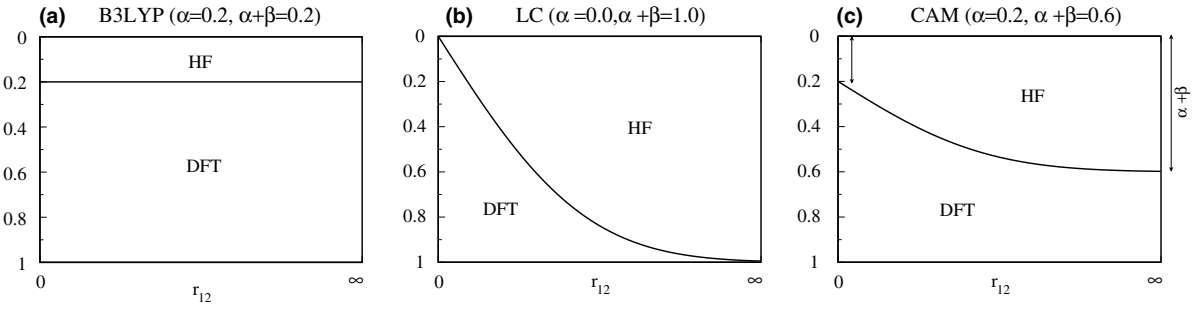

Fig. 2. Schematic plots of the contributions to exchange from r_{12}^{-1}, apportioned into DFT and HF, for: (a) B3LYP, (b) LC, and (c) CAM.

correlation functionals examined in this study. The Becke 1988 exchange functional is used in all of the LC and CAM functionals, and is mixed with the HF exchange according to Eq. (7). For the partner correlation functionals, we use the OP correlation functional, the Lee–Yang–Parr (LYP) [19], and the correlation functional employed in B3LYP, which is 0.19 VWN5 + 0.81 LYP, where the VWN5 functional is the local correlation functional of Vosko, Wilk and Nusair (VWN) [20] parameterized with the data of Ceperley and Alder [21]. Note that this is different to the standard B3LYP implemented in GAUSSIAN which uses VWN1 instead of VWN5 [18], we refer to this functional as B3LYP(G). The possible combinations of the exchange–correlation functionals are termed CAM-BOP, CAM-BLYP, CAM-B3LYP, LC-BOP, and LC-BLYP. For the parameter μ, the same value is used as in Tawada's study [1], $\mu = 0.33$. The parameter α, which determines the contribution of the HF exchange at the short-range region, was chosen to be 0.2 for the three functionals, CAM-BOP, CAM-BLYP, and CAM-B3LYP. We vary the parameter β so that the HF exchange could contribute to the long-range region with $\alpha + \beta = 0.6, 0.8$, or 1.0 for three functionals.

We compare the present functionals with four kinds of the widely used, well-examined exchange–correlation functionals, HCTH/93 [22], BLYP, B3LYP(G) (VWN1), and B3LYP (VWN5). We used the INTEGRA [23] as a part of the UTCHEM 2004 program package [24,25] to carry out Kohn–Sham self-consistent field (KS-SCF) calculations with the LC and CAM methods. The KS-SCF calculations with the standard BLYP, HCTH, B3LYP(G), and B3LYP were performed using NWCHEM program package version 4.5 [26].

4. Results

4.1. Atomization energies, ionization potentials, and atomic energies

We calculated 53 atomization energies and 22 ionization potentials from the molecules of the G2 set [27,28]. All calculations were performed with sufficiently accurate correlation-consistent aug-cc-pVQZ Gaussian basis sets. Tables 2 and 3 show the statistical data for atomization energies and ionization potentials with comparison to the experimental data, which are taken

Table 1
Summary of the exchange–correlation functionals

Name	Exchange functional	α	$\alpha + \beta$	Additional exchange	Correlation functional
LC-BOP	Becke88	0.0	1.0		OP
LC-BLYP	Becke88	0.0	1.0		LYP
CAM-BOP	Becke88	0.2	1.0		OP
			0.8		
			0.6		
CAM-BLYP	Becke88	0.2	1.0		LYP
			0.8		
			0.6		
CAM-B3LYP	Becke88	0.2	1.0		0.19 VWN5 + 0.81 LYP
			0.8		
			0.6		
B3LYP(G)	Slater	0.2	0.2	0.72 ΔBecke88	0.19 VWN1(RPA) + 0.81 LYP
B3LYP	Slater	0.2	0.2	0.72 ΔBecke88	0.19 VWN5 + 0.81 LYP
BLYP	Becke88	0.0	0.0		LYP
HCTH	xHCTH	0.0	0.0		cHCTH

along with zero point energies from [2,29]. Table 4 summarizes the atomic energy data of the first-row atoms H through Ne with comparison to the exact energies [2].

Within the standard exchange–correlation functionals, B3LYP(G) gives the smallest errors for the atomization energies with 2.54 kcal mol^{-1} for the mean absolute error (MAE) and 3.38 kcal mol^{-1} for the root mean square deviation (RMS). The HCTH functional gives the best performance for the ionization potentials within the standard functionals with 0.154 eV for MAE and 0.187 eV for RMS. B3LYP performs best for the atomization energies with 0.005E_h for both MAE and RMS.

The LC-based exchange–correlation functionals, LC-BOP and LC-BLYP, enormously overestimate the atomization energies with MAEs of 6–7 kcal mol^{-1} and RMS errors of 8–9 kcal mol^{-1}, while they perform comparably well for computing ionization potentials. Both of the LC functionals systematically overestimate the total atomic energies of H–Ne with an RMS of 0.09–0.13 E_h.

As for the CAM exchange–correlation functionals, the errors of the atomization energies are significantly improved compared to the LC method by setting $\alpha = 0.2$ for CAM-BOP, CAM-BLYP and CAM-B3LYP. For ionization energies, the CAM functionals are also better than the LC functionals. The CAM-BOP and CAM-BLYP functionals systematically overestimate the total atomic energies of H–Ne with a MAE of 0.069–0.030 E_h. The inclusion of the VWN5 correlation contribution into the LYP functional greatly reduces these errors to within an acceptable level. However, the atomization energy errors deteriorate by 0.1–0.3 kcal mol^{-1} with the inclusion of VWN5. We consider that due to the prevalence of hydrogen in chemical systems, the good reproduction of the total atomic energies, hydrogen in particular, is more important than the slight loss in quality of the atomization and ionization energies.

Table 2
Statistical data for atomization energies (kcal mol^{-1}) of the small G2 set (53 molecules) with aug-cc-pVQZ Gaussian basis sets

	α	$\alpha+\beta$	MAE	RMS	Maximum deviation (−)	Maximum deviation (+)
LC-BOP	0.0	1.0	9.19	11.22	−4.37 (Li_2)	25.47 (CO_2)
LC-BLYP	0.0	1.0	9.48	12.07	−3.23 (H_2)	29.64 (CO_2)
CAM-BOP	0.2	1.0	4.13	5.01	−8.98 (CN)	10.34 (N_2H_4)
		0.8	3.21	4.05	−9.33 (SO_2)	8.62 (BeH)
		0.6	2.93	3.95	−13.12 (SO_2)	8.58 (BeH)
CAM-BLYP	0.2	1.0	3.90	4.77	−7.00 (P_2)	13.66 (N_2H_4)
		0.8	2.77	3.51	−6.95 (CS)	9.96 (N_2H_4)
		0.6	2.28	3.15	−10.21 (SO_2)	7.60 (BeH)
CAM-B3LYP	0.2	1.0	3.99	4.87	−8.29 (P_2)	13.37 (N_2H_4)
		0.8	2.97	3.79	−9.03 (SO_2)	9.68 (N_2H_4)
		0.6	2.62	3.59	−12.82 (SO_2)	8.33 (BeH)
B3LYP(G)	0.2	0.2	2.54	3.38	−12.01 (SO_2)	8.33 (BeH)
B3LYP	0.2	0.2	2.68	3.58	−13.48 (SO_2)	8.21 (BeH)
BLYP	0.0	0.0	4.51	5.87	−10.42 (C_2H_6)	15.39 (O_2)
HCTH	0.0	0.0	3.50	4.76	−9.59 (C_2H_6)	14.96 (O_2)

Table 3
Statistical data for ionization potentials (eV) of the small G2 set (22 molecules) with aug-cc-pVQZ Gaussian basis sets

	α	$\alpha+\beta$	MAE	RMS	Maximum deviation (−)	Maximum deviation (+)
LC-BOP	0.0	1.0	0.192	0.220	−0.312 (Be)	0.386 (F)
LC-BLYP	0.0	1.0	0.230	0.272	−0.245 (Be)	0.552 (O)
CAM-BOP	0.2	1.0	0.166	0.203	−0.337 (Be)	0.488 (N_2)
		0.8	0.158	0.189	−0.358 (Be)	0.367 (N_2)
		0.6	0.153	0.185	−0.375 (Be)	0.291 (O_2)
CAM-BLYP	0.2	1.0	0.195	0.245	−0.272 (Be)	0.558 (N_2)
		0.8	0.185	0.225	−0.291 (Be)	0.446 (O_2)
		0.6	0.178	0.213	−0.311 (Be)	0.408 (O_2)
CAM-B3LYP	0.2	1.0	0.243	0.301	−0.179 (Be)	0.658 (N_2)
		0.8	0.218	0.273	−0.199 (Be)	0.537 (N_2)
		0.6	0.202	0.249	−0.223 (P_2)	0.499 (O_2)
B3LYP(G)	0.2	0.2	0.209	0.254	−0.210 (Be)	0.532 (O)
B3LYP	0.2	0.2	0.169	0.206	−0.293 (Be)	0.423 (O)
BLYP	0.0	0.0	0.208	0.250	−0.459 (Cl_2)	0.544 (O)
HCTH	0.0	0.0	0.154	0.187	−0.359 (Cl_2)	0.340 (N)

Table 4
Statistical data for total atomic energies (hartree) of H–Ne with aug-cc-pVQZ Gaussian basis sets

	α	$\alpha+\beta$	MAE	RMS	Maximum deviation (−)	Maximum deviation (+)	Deviation H
LC-BOP	0.0	1.0	0.084	0.093	–	0.134 (Ne)	0.0091
LC-BLYP	0.0	1.0	0.085	0.128	–	0.128 (Ne)	0.0091
CAM-BOP	0.2	1.0	0.068	0.075	–	0.112 (Ne)	0.0075
		0.8	0.049	0.054	–	0.080 (Ne)	0.0061
		0.6	0.030	0.049	–	0.049 (Be)	0.0047
CAM-BLYP	0.2	1.0	0.069	0.075	–	0.107 (Ne)	0.0075
		0.8	0.050	0.054	–	0.075 (Ne)	0.0061
		0.6	0.031	0.034	–	0.043 (Ne)	0.0047
CAM-B3LYP	0.2	1.0	0.033	0.035	–	0.045 (Be)	0.0034
		0.8	0.014	0.017	–	0.029 (Be)	0.0019
		0.6	0.009	0.013	−0.025 (Ne)	0.013 (Be)	0.0005
B3LYP(G)	0.2	0.2	0.019	0.023	−0.040 (Ne)	–	−0.0024
B3LYP	0.2	0.2	0.005	0.005	−0.006 (F)	0.009 (Be)	0.0010
BLYP	0.0	0.0	0.011	0.016	−0.031 (F)	0.007 (Be)	0.0021
HCTH	0.0	0.0	0.008	0.010	−0.019 (Ne)	0.004 (C)	−0.0064

Increasing the ratio of the Becke 88 exchange contribution at long-range reduces the errors of the atomization, ionization and the total atomic energies. For instance, the CAM-BLYP with $\alpha = 0.2$ and $\alpha+\beta = 0.6$ is better by 1.62 kcal mol^{-1} for MAE and RMS than that with $\alpha = 0.2$ and $\alpha+\beta = 1.0$. The maximum deviations are also reduced. While the CAM-BLYP method with $\alpha = 0.2$ and $\alpha+\beta = 0.6$ gives the smallest errors for the atomization energies of the three CAM functionals with a MAE of 2.28 kcal mol^{-1}, and CAM-BOP with $\alpha = 0.2$ and $\alpha+\beta = 0.6$ gives the best ionization energies with an MAE of 0.153 eV, we recommend CAM-B3LYP due to its success in reproducing total atomic energies.

We find that the optimal values for the two parameters α and β of CAM-B3LYP which yield the smallest errors for the atomization energies, are found to be

$$\alpha = 0.19 \text{ and } \beta = 0.46, \quad (\alpha+\beta = 0.65). \tag{9}$$

This functional yields results comparable to those of B3LYP for the atomization energies, ionization potentials and total atomic energies (Table 5). The sum $\alpha+\beta$ is rather crucial, because it gives the asymptotic coefficient of $-r^{-1}$. If we set $\alpha+\beta = 0.8$, (i.e., 0.15 more HF exchange at the long-range) we find optimal values to be

$$\alpha = 0.23 \quad \text{and} \quad \beta = 0.57, \tag{10}$$

for CAM-B3LYP. In Section 4.2, we use these two sets of α and β to investigate how the long-range HF exchange interaction effects the charge transfer excitations in TDDFT calculations. Table 5 summarizes the atomization energies, ionization potentials, total atomic energies with the above two forms of CAM-B3LYP. Both

Table 5
Statistical data for atomization energies (kcal mol^{-1}) (with 53 molecules), ionization potentials (eV) (with 22 atoms and molecules), and total atomic energies (hartrees) (with H atom through Ne atom) from the small G2 set using CAM-B3LYP with $\alpha+\beta = 0.65, 0.8$, compared to B3LYP and LC-BLYP with aug-cc-pVQZ Gaussian basis set

Name	α	$\alpha+\beta$	MAE	RMS	Maximum deviation (−)	Maximum deviation (+)
Atomization energy (kcal mol^{-1})						
CAM-B3LYP	0.19	0.65	2.53	3.46	−10.79 (SO_2)	8.34 (BeH)
	0.23	0.8	2.91	3.88	−12.25 (SO_2)	8.41 (BeH)
B3LYP	0.2	0.2	2.68	3.58	−13.48 (SO_2)	8.21 (BeH)
LC-BLYP	0.0	1.0	9.48	12.07	−3.23 (H_2)	29.64 (CO_2)
Ionization potentials (eV)						
CAM-B3LYP	0.19	0.65	0.208	0.256	−0.212 (Be)	0.503 (O_2)
	0.23	0.8	0.213	0.271	−0.203 (Be)	0.563 (N_2)
B3LYP	0.2	0.2	0.169	0.206	−0.293 (Be)	0.423 (O)
LC-BLYP	0.0	1.0	0.230	0.272	−0.245 (Be)	0.552 (O)
Total atomic energies (hartree)						
CAM-B3LYP[a]	0.19	0.65	0.009	0.011	−0.017 (F)	0.018 (Be)
	0.23	0.8	0.012	0.015	–	0.026 (Be)
B3LYP	0.2	0.2	0.005	0.005	−0.006 (F)	0.009 (Be)
LC-BLYP	0.0	1.0	0.085	0.128	–	0.128 (Ne)

[a] Deviation of H atom from the exact atomic energy (hartrees): 0.0010 (CAM-B3LYP $\alpha = 0.19$, $\alpha+\beta = 0.65$), 0.0017 (CAM-B3LYP $\alpha = 0.23$, $\alpha+\beta = 0.80$).

Table 6
The electronic spectrum (eV) of a dipeptide ($C_5N_2O_2H_{10}$) with the basis sets TZ2P (5s4p2d on first row; 3s2p on H)

		Band	CASPT2	AC-HCTH	B3LYP	BLYP	LC-BLYP	CAM-B3LYP $\alpha = 0.19$, $\alpha + \beta = 0.65$	CAM-B3LYP $\alpha = 0.23$, $\alpha + \beta = 0.8$
			Tozer et al. [7]			Yanai et al. (this work)			
$^1A''$	$n_1 \rightarrow \pi_1^*$	W_1	5.61 (0.0006)	5.43 (0.0009)	5.49 (0.0013)	5.34 (0.0009)	5.56 (0.0007)	5.65 (0.0008)	5.72 (0.0008)
$^1A''$	$n_2 \rightarrow \pi_2^*$	W_2	5.82 (0.0006)	5.70 (0.0005)	5.73 (0.0009)	5.62 (0.0005)	5.80 (0.0003)	5.88 (0.0004)	5.95 (0.0004)
$^1A''$	$n_1 \rightarrow \pi_2^*$	CT	7.92 (0.0000)	4.67 (0.0000)	6.24 (0.0000)	4.60 (0.0002)	8.38 (0.0003)	7.88 (0.0001)	8.58 (0.0001)
$^1A'$	$\pi_1 \rightarrow \pi_1^*$	NV_1	6.32 (0.2737)	6.98 (0.0238)	7.19 (0.0645)	–	7.57 (0.0830)	7.52 (0.0869)	7.77 (0.0816)
$^1A'$	$\pi_2 \rightarrow \pi_2^*$	NV_2	6.29 (0.3205)	6.87 (0.2863)	7.23 (0.2704)	6.82 (0.2397)	7.26 (0.3437)	7.32 (0.3555)	7.43 (0.3572)
$^1A'$	$\pi_1 \rightarrow \pi_2^*$	CT	6.92 (0.1168)	5.16 (0.0043)	6.06 (0.0029)	5.07 (0.0041)	7.02 (0.0430)	6.94 (0.0184)	7.24 (0.0399)

Oscillator strengths within parentheses.

forms are similar in quality to B3LYP, and are a great improvement over LC-BLYP.

4.2. Charge transfer excitations in the dipeptide model

Excited state calculations with TDDFT were performed on a glycine dipeptide model system, which was previously studied by Tozer and co-workers [7]. We used the same geometry with the same basis sets TZ2P (5s4p2d on first row; 3s2p on H) as used in Tozer's study. Table 6 lists the excitation energies and the oscillator strengths. It is to be noted that the $n \rightarrow \pi^*$ excitations within the same fragment are well produced by all the DFT methods, when compared to the highly accurate multireference perturbation calculation with CASPT2 [30].

The charge transfer excitations of $n \rightarrow \pi^*$ and $\pi \rightarrow \pi^*$ between different fragments are very poorly predicted by the DFT calculations with the standard exchange–correlation functionals, in particular the BLYP for $n \rightarrow \pi^*$ is much lower by 3.3 eV than CASPT2. B3LYP yields values 1.7 eV lower than CASPT2. This means that the $0.2r^{-1}$ contribution via HF exchange in B3LYP improves the charge transfer excitations. Tozer and Handy's asymptotic correction does not work for these states.

It is very encouraging that the CAM-B3LYP with $\alpha = 0.19$ and $\alpha + \beta = 0.65$ predictions of charge transfer excitations are in excellent agreement with the CASPT2 results. It is not surprising that the LC-BLYP method brings the charge transfer excitations into much better agreement with CASPT2 than the standard DFT exchange–correlation functionals, because of the $1.0r^{-1}$ asymptotic form through the HF exchange. The CAM-B3LYP functional with $\alpha = 0.23$ and $\alpha + \beta = 0.8$ yields almost comparable results to LC-BLYP. By comparison between the two sets of results obtained with CAM-B3LYP, we see that the long-range contribution of the HF exchange interaction has a large impact on the charge transfer excitations as compared with the other calculated excitations.

The predictions for the $\pi \rightarrow \pi^*$ excitation within the same fragment are overestimated by all the DFT methods. A clue to the problem lies in the oscillator strengths. In DFT $\pi_2 \rightarrow \pi_2^*$ is dominant, whereas $\pi_1 \rightarrow \pi_1^*$ and $\pi_2 \rightarrow \pi_2^*$ have equal strengths in CASPT2. If the problem is truly multiconfigurational, then DFT will fail. This is the most plausible explanation.

5. Conclusions

The recent work by Tsuneda and co-workers [1,10] has shown how DFT studies can now be performed to a useful accuracy for polarizability of long chains, excitations to Rydberg states and charge transfer excita-

tions. Previously DFT calculations using GGA functionals (BLYP) and hybrid functionals (B3LYP) have been frequently used for energetic studies and structural studies. A combination of the two clearly goes a long way for the provision of a very useful computational chemistry methodology.

We are suggesting that the CAM-B3LYP functional presented in this Letter meets these criteria. In the CAM-B3LYP functional, we have replaced the Becke parameter α by two parameters α, β for mixing Becke 1988 exchange and HF exchange, with μ describing the conversion from one to the other through Eq. (7). Our best functional uses $\alpha = 0.19$, $\alpha + \beta = 0.65$ and $\mu = 0.33$ (Tawada's value). We used Becke's VWN5/LYP mixing parameter ($= 0.19$) for the correlation functional without adjustment. Our calculations have shown that this functional predicts energetic quantities to the accuracy of B3LYP. Our first investigations on charge transfer energies suggest that it is possible to achieve chemical accuracy (0.1 eV). The cost for the implementation of this functional is no more severe than that required for B3LYP (within a factor of 2 for computing two-electron integrals). This functional is a hybrid functional with improved long-range properties.

Acknowledgements

We acknowledge Dr. R.J. Harrison for the encouragement of this work, the use of the computer resources at ORNL, and arranging TY's visit to NCH's group at Cambridge. We would like to thank Professor K. Hirao, Dr. T. Tsuneda, Y. Tawada and Dr. M. Sprik for valuable discussions, Dr. D.J. Tozer for providing us with input files for the dipeptide, Dr. A.J. Cohen for input files of G2 set molecules. TY thanks Dr. S. Hirata for teaching TY the implementation of TDDFT, and M. Kamiya for his DFT quadrature code in INTEGRA of UTCHEM. NWCHEM Version 4.5, as developed and distributed by Pacific Northwest National Laboratory, P.O. Box 999, Richland, Washington 99352 USA, funded by the US Department of Energy, was used to obtain the DFT results.

References

[1] Y. Tawada, T. Tsuneda, S. Yanagisawa, T. Yanai, K. Hirao, J. Chem. Phys. 120, in press.
[2] A.D. Becke, J. Chem. Phys. 98 (1993) 5648.
[3] P.J. Stephens, J.F. Devlin, C.F. Chabalowski, M.J. Frisch, J. Chem. Phys. 98 (1993) 11623.
[4] M.E. Casida, in: D.P. Chong (Ed.), Recent Advances in Density Functional Methods, vol. 1, World Scientific, Singapore, 1995.
[5] R. Bauernschmitt, R. Ahlrichs, Chem. Phys. Lett. 256 (1996) 454.
[6] D.J. Tozer, N.C. Handy, J. Chem. Phys. 109 (1998) 10180.
[7] D.J. Tozer, R.D. Amos, N.C. Handy, B.O. Roos, L. Serrano-Andres, Mol. Phys. 97 (1999) 859.
[8] A. Dreuw, J.L. Weisman, M. Head-Gordon, J. Chem. Phys. 119 (2003) 2943.
[9] L. Bernasconi, M. Sprik, J. Hutter, J. Chem. Phys. 119 (2003) 12417.
[10] H. Iikura, T. Tsuneda, T. Yanai, K. Hirao, J. Chem. Phys. 115 (2001) 3540.
[11] A. Savin, in: J.M. Seminario (Ed.), Recent Developments and Applications of Modern Density Functional Theory, Elsevier, Amsterdam, 1996.
[12] P.M.W. Gill, R.D. Adamson, J.A. Pople, Mol. Phys. 88 (1996) 1005.
[13] T. Leiniger, H. Stoll, H.-J. Werner, A. Savin, Chem. Phys. Lett. 275 (1997) 151.
[14] A.D. Becke, Phys. Rev. A 38 (1988) 3098.
[15] J.P. Perdew, K. Burke, M. Ernzerhof, Phys. Rev. Lett. 77 (1996) 3865.
[16] T. Tsuneda, T. Suzumura, K. Hirao, J. Chem. Phys. 110 (1999) 10664.
[17] M. Kamiya, T. Tsuneda, K. Hirao, J. Chem. Phys. 117 (2002) 6010.
[18] R.H. Hertwig, W. Koch, Chem. Phys. Lett. 268 (1997) 345.
[19] C. Lee, W. Yang, R.G. Parr, Phys. Rev. B 37 (1988) 785.
[20] S.J. Vosko, L. Wilk, M. Nusair, Can. J. Phys. 58 (1980) 1200.
[21] D.M. Ceperley, B.J. Alder, Phys. Rev. Lett. 45 (1980) 566.
[22] F.A. Hamprecht, A.J. Cohen, D.J. Tozer, N.C. Handy, J. Chem. Phys. 109 (1998) 6264.
[23] H. Iikura, H. Inoue, M. Kamiya, Y. Kawashima, T. Nakajima, Y. Nakao, K. Nakayama, H. Sekino, K. Sorakubo, T. Tawada, T. Tsuneda, K. Yagi, S. Yanagisawa, T. Yanai, K. Hirao, INTEGRA, Department of Applied Chemistry, School of Engineering, University of Tokyo, Japan.
[24] T. Yanai, M. Kamiya, Y. Kawashima, T. Nakajima, H. Nakano, Y. Nakao, H. Sekino, J. Paulovic, T. Tsuneda, S. Yanagisawa, K. Hirao, UTCHEM 2004, Department of Applied Chemistry, School of Engineering, University of Tokyo, Japan.
[25] T. Yanai, H. Nakano, T. Nakajima, T. Tsuneda, S. Hirata, Y. Kawashima, Y. Nakao, M. Kamiya, H. Sekino, K. Hirao, in: Computational Science – ICC 2003, Lecture Notes in Computer Science, Springer, 2003, p. 84.
[26] High Performance Computational Chemistry Group, NWCHEM, A Computational Chemistry Package for Parallel Computers, Version 4.5, Pacific National Laboratory, Richland, Washington 99352, USA, 2003.
[27] L.A. Curtiss, K. Raghavachari, P.C. Redfern, J.A. Pople, J. Chem. Phys. 106 (1997) 1063.
[28] N.C. Handy, D.J. Tozer, Mol. Phys. 94 (1998) 707, References of molecular bond lengths and bond angles therein.
[29] D. Feller, K.A. Peterson, J. Chem. Phys. 110 (1999) 8384.
[30] K. Andersson, P.-Å. Malmqvist, B.O. Roos, A.J. Sadlej, K. Wolinski, J. Phys. Chem. 94 (1990) 5483.